Optics Letters

Effective method to study the thickness-dependent dielectric functions of nanometal thin film

Er-Tao Hu,[1,3] Qing-Yuan Cai,[2] Rong-Jun Zhang,[3,5] Yan-Feng Wei,[2] Wen-Chao Zhou,[4] Song-You Wang,[3] Yu-Xiang Zheng,[3] Wei Wei,[1,6] and Liang-Yao Chen[3]

[1]School of Optoelectronic Engineering, Nanjing University of Posts and Telecommunications, Nanjing 210023, China
[2]Shanghai Institute of Technical Physics, Chinese Academy of Sciences, Shanghai 200083, China
[3]Department of Optical Science and Engineering, Fudan University, Shanghai 200433, China
[4]State Key Laboratory of Applied Optics, Changchun Institute of Optics, Fine Mechanics and Physics, Chinese Academy of Sciences, Changchun, Jilin 130033, China
[5]e-mail: rjzhang@fudan.edu.cn
[6]e-mail: iamww@fudan.edu.cn

Received 2 August 2016; revised 24 September 2016; accepted 27 September 2016; posted 28 September 2016 (Doc. ID 272894); published 21 October 2016

A new method for measuring the dielectric functions change with the thickness of nanometal thin films was proposed. To confirm the accuracy and reliability of the method, a nano-thin wedge-shaped gold (Au) film with continuously varied thicknesses was designed and prepared on K9 glass by direct-current-sputtering (DC-sputtering). The thicknesses and the dielectric functions in the wavelength range of 300–1100 nm of the nano-thin Au films were obtained by fitting the ellipsometric parameters with the Drude and critical points model. Results show that while the real part of the dielectric function (ε_1) changes marginally with increasing film thickness, the imaginary part (ε_2) decreases drastically with the film thickness, approaching a stable value when the film thickness increases up to about 42 nm. This method is particularly useful in the study of thickness-dependent optical properties of nano-thin film. © 2016 Optical Society of America

OCIS codes: (310.6860) Thin films, optical properties; (290.3030) Index measurements.

http://dx.doi.org/10.1364/OL.41.004907

With the recent advances in micro- and nano-fabrication technologies, nanometric thin film has received extensive attention in the fields of nanoelectronics, optoelectronics, and photonics, including transparent electrodes [1], antireflection coatings [2], optical metamaterials [3], and nanoplasmonic devices for biochemical sensing [4,5]. Though the optical constants of the most materials has been reported and summarized in Palik's optical database [6], it is not applicable to nano-thin films with thicknesses under several tens of nanometers because it has been proved that the optical constants of thin films are dependent on the film thickness [4,7,8]. Obvious deviations with the experimental results were found when bulk optical constants were used in the simulations [9], especially when the device's performance is sensitive to the dielectric functions of their components. Hence, a detailed study of the dielectric functions of nano-thin Au film is very essential for its wide optical and electrical applications.

Generally, optical constants can be obtained by spectroscopic ellipsometry (SE) [7,8], the surface plasmon resonance technique [10], and the reflectance and transmittance method [11]. However, the SE technique is the most used method in the determination of the energy dispersion of complex dielectric functions, $\varepsilon(\omega) = \varepsilon_1(\omega) + \varepsilon_2(\omega)$ of thin films in high accuracy due to its surface sensitive and nondestructive feature. For SE measurements, to evaluate the influence of the film thickness on the dielectric functions, usually lots of samples with various thicknesses need to be deposited and measured. It will lead to the difficulty in ensuring the identical deposition and measurement conditions of samples with different thicknesses, which will induce unavoidable errors in the determination of the thickness influence on the optical constants.

To overcome the disadvantages of traditional multiple-sample measurements, a new method was proposed for measuring the dielectric functions change with the thickness of the nanometal thin films in this Letter. A novel of wedge-shaped nano-thin Au film on K9 glass with continuously varied thicknesses was designed and fabricated by a DC-sputtering method. The dielectric functions of the nano-thin Au film were obtained by the spectroscopic ellipsometer (SE). Afterward, the influences of the film thickness on the dielectric functions and free-electron relaxation time were discussed.

The nano-thin Au film with the target purity of 99.99% was DC-sputtered on the double-polished K9 wedge-shaped glass with an angle of about 2° in the Leybold LAB600 SP chamber at room temperature. Prior to evaporation, the K9 substrate was ultrasonically cleaned using acetone, ethanol, and deionized water for 10 min, respectively; then it was dried under a nitrogen atmosphere. The target–substrate distance was 9 cm. The working pressure, discharge voltage, current, and power were fixed at 3.0×10^{-3} mbar, 428 V, 0.07 A, and 30 W,

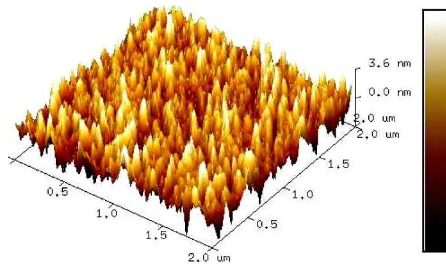

Fig. 1. AFM image of the nano-thin Au film on K9 substrate.

respectively. In this Letter, a mask was driven by a stepping motor at a constant velocity of about 11.4 μm/s during the deposition process to obtain the wedge-shaped sample [8].

The surface morphology of the sample at different positions was characterized by atomic force microscopy (AFM Bruker Multimode-8) in the contact mode with the scanning area of $2 \times 2\ \mu m^2$, with one of the results showing in Fig. 1. It indicates that the surface roughness is nearly uniform for all the measured areas with $R_q \approx 1.0$ nm (root mean square of surface roughness), which is in favor of the ellipsometry measurements.

The variable-angle spectroscopic ellipsometer (J.A. Woollam VASE) was used to simultaneously extract both the thickness and complex dielectric functions of the thin Au film at different positions of the wedge-shaped nano-thin Au film (from positions 1 to 12, with the distance between the adjacent positions along the measuring direction of about 1 mm). A focused beam with the measured area of about 200 μm was used to overcome the restriction of uniform characteristics within a relatively large region of the typical probe beam of SE.

Ellipsometric parameters (Ψ, Δ) were obtained over the wavelength range of 300–1100 nm at three different incident angles of 65°, 70°, and 75°, respectively. To avoid the influence of the prolongation of the beam size along the direction of the incident light on the thickness of the Au thin film due to the different incident angles, the incident plane was perpendicular to the sample surface. Details can be found in our previous work [8].

The values of ellipsometric parameters (Ψ, Δ) are defined from the ratio of the amplitude reflection coefficients for p- and s-polarizations [12]:

$$\rho = \tan \Psi \exp(i\Delta) = r_p / r_s, \tag{1}$$

where r_p and r_s represent the reflectance of the p- and s-polarizations, respectively.

To obtain the real film thickness and dielectric functions, an accurate theoretical dispersion model must be chosen. For metal, a Drude and Lorentz (DL) model, as shown in Eq. (2) [13], was always used to depict the free electron intra-band transitions in the infrared frequency region and bond electron inter-band transitions in the visible/near-UV region, respectively:

$$\varepsilon = \varepsilon_\infty - \frac{E_p^2}{E(E + i\Gamma_p)} + \sum_{j=1}^{n} \frac{A_j^2}{E_j^2 - E^2 + iE\Gamma_j}. \tag{2}$$

In Eq. (2), ε, ε_∞, E_p, and Γ_p are the complex dielectric function, the high-frequency dielectric constant, the plasma frequency, and the Drude broadening, respectively. Furthermore, A_j, E_j, and Γ_j are the oscillator strength, oscillator energy, and oscillator damping, respectively. In our previous work [8], the DL model was utilized to predict the optical dispersion properties of the titanium (Ti) thin film. However, it has been found that the DL model faces limitations in predicting the inter-band transitions of the Au in the visible/near-UV region due to the somewhat asymmetric transition line shape of the Au which will add "artificial" and unphysical parameters in the DL model [14]. By considering the two inter-band transitions in the visible/near-UV range, Etchegoin *et al.*, proposed an analytic model [14] called the Drude and critical points (DCP) model as follows:

$$\varepsilon = \varepsilon_\infty - \frac{E_p^2}{E(E + i\Gamma_p)} + \frac{A_1 e^{i\phi_1}}{E_1 - E - i\Gamma_1} + \frac{A_1 e^{-i\phi_1}}{E_1 + E + i\Gamma_1} + \frac{A_2 e^{i\phi_2}}{E_2 - E - i\Gamma_2} + \frac{A_2 e^{-i\phi_2}}{E_2 + E + i\Gamma_2}, \tag{3}$$

where the two critical points correspond to the two inter-band transitions in the visible/near-UV region of the Au. Compared with Eq. (2), a phase parameter ϕ is added in the DCP model to account for the band-edge effects. The expression is consistent with the Kramers–Kronig relation. Note that the DCP model does not satisfy the "plasma sum rule," but it can be used over a finite frequency range [14].

To accurately characterize the optical dispersion properties of the Au nano-thin films at different thicknesses in the wavelength range of 300–1100 nm, the DCP model was chosen in this case to fit the experimental data. The difference between the measurements and the fitting results is defined by the root mean square error (RMSE) [7]:

$$\mathrm{RMSE} = \sqrt{\frac{1}{2N - M} \sum_{i=1}^{N} \left[\left(\frac{\Psi_i^{\mathrm{mod}} - \Psi_i^{\mathrm{exp}}}{\sigma_{\Psi,i}^{\mathrm{exp}}} \right)^2 + \left(\frac{\Delta_i^{\mathrm{mod}} - \Delta_i^{\mathrm{exp}}}{\sigma_{\Delta,i}^{\mathrm{exp}}} \right)^2 \right]}, \tag{4}$$

where N is the number of the experimental points, M is the number of parameters, σ is the standard deviation, and the superscripts mod and exp refer to the modeled and measured data, respectively.

A four-phase model consisting of air/roughness layer/Au layer/K9 glass was employed in the SE parameter fitting process. For the Au layer, the DCP model was chosen. In Eq. (3), ε_∞ is the value of the dielectric functions at infinite energy, which is assumed to be 1 in all fittings. The Bruggeman effective medium approximation model [15] was used to depict the roughness layer which is consistent with the Au and void. To reduce the fitting parameters, the void fraction was set to 50%, and the rough layer thickness was set to 1.0 nm. To exclude the influence of the reflected light from the rear surface of the K9 glass, a wedge-shaped K9 substrate was used with its optical constants measured in advance.

The ellipsometric parameters with the incident angle of 70° at different measured positions (corresponding to the different thicknesses of the nano-thin Au film) were presented in Fig. 2. It shows that the fitting of the Au films at different film thicknesses presents a good agreement with the experimental data in the entire measured spectral range at the three incident angles with the RMSE ≈ 0.18, which demonstrates that our fittings are accurate and reliable in the whole investigated spectrum range. It is evidenced that both the parameters Ψ and Δ increase with the film thickness, to be nearly unchanged when

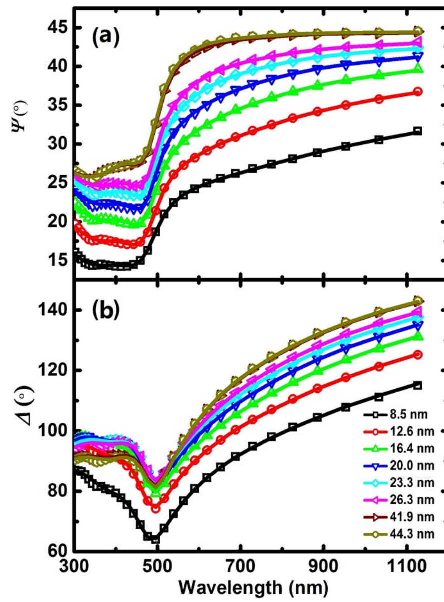

Fig. 2. Measured (*symbol*) and fitting (*line*) ellipsometry data Ψ and Δ of the Au film for various thicknesses at an incident angle of 70°.

the film thickness increases to 41.9 nm, indicating the change trend of the dielectric functions with the Au film thickness.

The fitting parameters are listed in Table 1. For the Au, the two inter-band transitions are located at the L and X symmetry points, with the calculated energy gap of about 4.0 and 2.5 eV, respectively [16]. Consistent results have been produced from our SE fitting ($E_1 \approx 3.35$ eV, $E_2 \approx 2.62$ eV). Similar results have been found in the literature [14], proving the accuracy of our fitting. The nearly unchanged plasma energy with the film thickness at a value of about 9.4 eV, is comparable with the data from [6,17]. The fitted film thickness changes from 8.5 to 44.3 nm. For thin Au films, it has been found that the thickness obtained from an ellipsometer is consistent with the result measured by transmission electron microscopy with an error of about 1.0 nm in the previous work [7].

The distance between adjacent positions along the measuring direction was about 1 mm. Hence, the thickness gradient was about 3.5 nm/mm along the measuring direction. In each measured area (≈200 μm), the Au film thickness difference is just about 0.7 nm. It is so small a value compared with the large measured region [8,18] that the film can be considered as uniform in the measured area. For simplicity, the fitting parameters for position 7, 8, 9, and 10 were not shown in the Table.

The real (ε_1) and imaginary (ε_2) parts of the dielectric functions of the Au nano-films are given in Fig. 3 with the data obtained from Palik [6] and Johnson and Christy [17] for comparison. A similar variation trend with a wavelength of our results with the references has been found. It proves that, with the wedge-shaped Au film sample, the intrinsic dielectric dispersion relations can be obtained due to the identical deposition and measuring conditions.

As is clearly shown in Fig. 3, ε_1 is almost uninfluenced by the film thickness, but ε_2 has a larger variation. Here, ε_1 seems to change little with the film thickness because the variation of ε_1 with wavelength is much larger than its change with the film thickness. It can also be found that when the film thickness increases up to 42 nm, both ε_1 and ε_2 are nearly uninfluenced by film thickness, indicating the bulk thickness of the Au film in this frequency region. When the film thickness is larger than the bulk electron mean free path of the Au (40 nm [19]), the contribution from film scattering will approach to that of bulk material, inducing the optical properties independent of the film thickness.

For ε_1, it is negative in the whole spectrum range for the film thickness investigated by us, indicating the continuous film morphology of our sample [20]. For the Au thin film, the critical thickness for the surface changes from granular to continuous is about 7 nm [20]. Hence, it is reasonable to regard the film at the measured area as continuous because of the thinnest film thickness focused by us is 8.5 nm.

From the fitting parameters, it can also be found that with the film thickness increasing from 8.5 to 41.9 nm, the free electron relaxation time $\tau = 1/\Gamma_p$ (Γ_p: Drude damping factor) increases monotonically, as depicted in Fig. 4. It proves that the metallic character of the Au thin film is enhanced with the increase of the film thickness. The result agrees well with the previous investigations [7] which can be understood from the fact that the scattering of boundaries and imperfection becomes more and more important as the film thickness is reduced. The surface scattering increases with the decreasing film thickness which, in turn, will make the Drude broadening larger. This will lead to the increase of ε_2, which is proportional to Γ_p at a longer wavelength ($\varepsilon_2 \sim \omega_p^2\Gamma_p/\omega^3$) [7]. When the film thickness gets even larger, to 44.3 nm, the relaxation time shows a stable value at 15.5 fs and will not be improved further.

Table 1. Fitting Parameters of Different Positions of the Nano-Thin Au Film by Using the DCP Model

Measured Position	**1**	**2**	**3**	**4**	**5**	**6**	**11**	**12**
Film Thickness (nm)	**8.5**	**12.6**	**16.4**	**20.0**	**23.3**	**26.3**	**41.9**	**44.3**
RMSE	0.14	0.16	0.17	0.18	0.17	0.18	0.18	0.18
E_p (eV)	9.33	9.37	9.41	9.43	9.45	9.48	9.40	9.39
$\Gamma_p(10^{-2}$ eV)	11.48	9.14	7.86	6.89	5.99	5.15	4.20	4.23
E_1 (eV)	2.61	2.64	2.64	2.63	2.63	2.62	2.62	2.62
A_1 (eV)	1.32	1.47	1.45	1.48	1.50	1.54	1.61	1.65
Γ_1 (eV)	0.40	0.41	0.40	0.39	0.39	0.39	0.39	0.40
ϕ_1	−1.13	−0.92	−0.94	−0.94	−0.95	−0.95	−0.92	−0.91
E_2 (eV)	3.40	3.35	3.35	3.35	3.31	3.30	3.36	3.38
A_2 (eV)	11.14	10.24	10.15	9.97	9.76	9.58	9.53	9.41
Γ_2 (eV)	1.95	1.72	1.67	1.64	1.60	1.57	1.52	1.50
ϕ_2	−0.72	−0.88	−0.89	−0.91	−0.95	−0.99	−1.00	−1.00

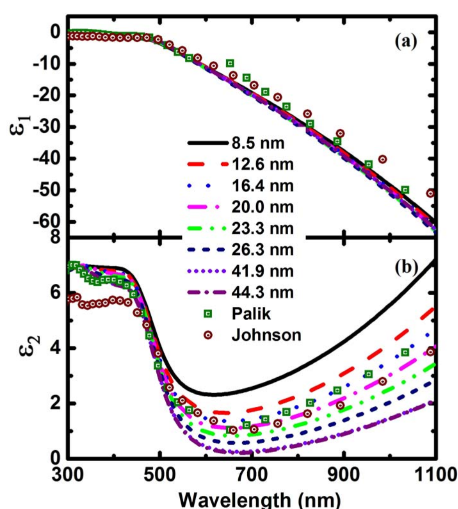

Fig. 3. (a) Real and (b) imaginary parts of the dielectric functions of the nano-thin Au film at different thicknesses.

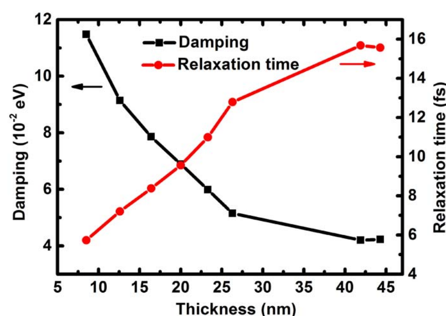

Fig. 4. Damping and free electron relaxation time for the Au at different film thicknesses.

It is consistent with the relaxation time of the bulk Au (14 ± 3 fs) [21].

In conclusion, a new method for measuring the dielectric functions change with the film thickness of nanometal thin films was proposed and confirmed by the Au film. The nano-thin Au film was designed and prepared by DC-sputtering to form a wedge shape with continuously varied thicknesses, which was employed to study the thickness influences on the dielectric functions. The single sample measurements can overcome the disadvantages of traditional multi-sample measurements. The DCP model was chosen to characterize the dispersion relations of nano-thin Au films with fitting results showing an extremely good agreement with the experimental ellipsometric parameters, illustrating the accuracy of obtained dielectric functions. Results reveal that while the real part of the dielectric function (ε_1) is nearly unchanged with the film thickness, the imaginary part (ε_2) decreases with increasing film thickness, which is mainly because of the reduced surface scattering in the thicker film. It is also found that the bulk thickness is about 42 nm for the Au thin film in the wavelength range of 300–1100 nm. The method provided in this Letter is demonstrated to be effective in the evaluation of the thickness effect on the optical properties of nano-thin films and can be used for many other materials as well.

Funding. National Natural Science Foundation of China (NSFC) (11674062, 61605089, 11174058, 11374055, 61275160); Science and Technology Commission of Shanghai Municipality (STCSM) (13ZR1463700); Chinese Academy of Sciences (CAS) (CX-75).

REFERENCES

1. M. S. R. Khan and A. Reza, Appl. Phys. A **54**, 204 (1992).
2. B. Gompf, J. Beister, T. Brandt, J. Pflaum, and M. Dressel, Opt. Lett. **32**, 1578 (2007).
3. A. V. Kildishev, A. Boltasseva, and V. M. Shalaev, Science **339**, 1232009 (2013).
4. P. Y. Kuryoz, L. V. Poperenko, and V. G. Kravets, Phys. Status Solidi A **210**, 2445 (2013).
5. H. Liu, B. Wang, E. S. Leong, P. Yang, Y. Zong, G. Si, J. Teng, and S. A. Maier, ACS Nano **4**, 3139 (2010).
6. E. D. Palik, *Handbook of Optical Constants of Solids* (Academic, 1998).
7. M. Y. Zhang, Z. Y. Wang, T. N. Zhang, Y. Zhang, R. J. Zhang, X. Chen, Y. Sun, Y. X. Zheng, S. Y. Wang, and L. Y. Chen, J. Nanophotonics **10**, 033009 (2016).
8. E. T. Hu, R. J. Zhang, Q. Y. Cai, Z. Y. Wang, J. P. Xu, Y. X. Zheng, S. Y. Wang, Y. F. Wei, R. Z. Huang, and L. Y. Chen, Appl. Phys. A **120**, 875 (2015).
9. N. Liu, M. Mesch, T. Weiss, M. Hentschel, and H. Giessen, Nano Lett. **10**, 2342 (2010).
10. O. Y. Posudievsky, A. V. Samoylov, E. R. Surovtseva, R. V. Khristosenko, A. L. Kukla, and Y. M. Shirshov, Thin Solid Films **516**, 6104 (2008).
11. X. Sun, R. Hong, H. Hou, Z. Fan, and J. Shao, Thin Solid Films **515**, 6962 (2007).
12. H. Fujiwara, *Spectroscopic Ellipsometry: Principles and Applications* (Wiley, 2007).
13. A. D. Rakic, A. B. Djurisic, J. M. Elazar, and M. L. Majewski, Appl. Opt. **37**, 5271 (1998).
14. P. G. Etchegoin, E. C. Le Ru, and M. Meyer, J. Chem. Phys. **125**, 164705 (2006).
15. D. E. Aspnes, Thin Solid Films **89**, 249 (1982).
16. D. Rioux, S. Vallières, S. Besner, P. Muñoz, E. Mazur, and M. Meunier, Adv. Opt. Mater. **2**, 176 (2013).
17. P. B. Johnson and R. W. Christy, Phys. Rev. B **6**, 4370 (1972).
18. D. Nečas, I. Ohlídal, and D. Franta, J. Opt. **13**, 085705 (2011).
19. W. Doliński, S. Mróz, J. Palczyński, B. Gruzza, P. Bondot, and A. Porte, Acta Phys. Pol. A **81**, 193 (1992).
20. M. Hövel, B. Gompf, and M. Dressel, Phys. Rev. B **81**, 1718 (2010).
21. R. L. Olmon, B. Slovick, T. W. Johnson, D. Shelton, S.-H. Oh, G. D. Boreman, and M. B. Raschke, Phys. Rev. B **86**, 235147 (2012).